nature neuroscience

Laterodorsal tegmentum interneuron subtypes oppositely regulate olfactory cue-induced innate fear

Hongbin Yang[1,5], Junhua Yang[1,5], Wang Xi[1], Sijia Hao[1], Benyan Luo[2], Xiaobin He[3], Liya Zhu[1], Huifang Lou[1], Yan-qin Yu[1], Fuqiang Xu[3,4], Shumin Duan[1] & Hao Wang[1]

Innate fear has a critical role in survival of animals. Unlike conditioned fear, the neuronal circuitry underlying innate fear is largely unknown. We found that the laterodorsal tegmentum (LDT) and lateral habenula (LHb) are specifically activated by the mouse predator odorant trimethylthiazoline (TMT). Using optogenetics to selectively stimulate GABAergic neurons in the LDT immediately produced fear-like responses (freezing, accelerated heart rate and increased serum corticosterone), whereas prolonged stimulation caused anxiety-like behaviors. Notably, although selective stimulation of parvalbumin (PV)-positive interneurons similarly induced fear-like responses, stimulation of somatostatin-positive interneurons or inhibition of PV neurons in the LDT suppressed TMT-induced fear-like responses without affecting conditioned fear. Finally, activation of LHb glutamatergic inputs to LDT interneurons was sufficient to generate fear-like responses. Thus, the LHb-LDT pathway is important for regulating olfactory cue–induced innate fear. Our results provide a potential target for therapeutic intervention for anxiety disorder.

Innate fear is a basic and natural mechanism by which animals and humans avoid danger. This emotion is trigged by a threat perceived through sensory stimuli, which usually causes a quick response, such as freezing, flight or hiding, and thus has a profound role in survival and health[1,2]. Abnormal innate fear in humans, particularly phobias and panic disorders[1–3], is strongly associated with anxiety disorders. The features of heritability and natural acquisition distinguish innate fear from conditioned fear. Unlike the innate fear circuitry, extensive studies have shown that the amygdala, hippocampus and prefrontal cortex are crucial for conditioned fear[4–6]. Emerging evidence suggests that distinct neuronal circuits are responsible for fear induced by different cues. For example, the lateral and central nuclei of the amygdala have a crucial role in conditioned fear, but not in the innate fear induced by an olfactory cue[7,8]. Although the cortical area of the amygdala has recently been shown to be responsible for innate fear induced by an olfactory cue[9], and a number of studies have reported the expression pattern of the immediate-early gene *c-fos* in the rodent brain in response to TMT or the odor of cat[10], the underlying neuronal circuitry is still largely unknown.

RESULTS

Activation of GABAergic interneurons in the LDT produces fear

To explore the neuronal circuitry for olfactory cue–induced innate fear in rodents, we first studied c-Fos protein expression in the whole brain when provoked by the pungent odor TMT. Previous studies have shown that TMT effectively induces fear behavior–like freezing in naive mice and can therefore be used to study the neurobiology of innate fear[8]. As a result of its unpleasant smell, we assumed that TMT would activate neuronal circuits in addition to those for innate fear, such as olfaction. Thus, as well as saline controls, we used β-mercaptoethanol (ME), which also has a pungent odor, but does not induce freezing behavior in mice, as a positive control. Compared with saline and ME stimuli, we found that TMT exposure specifically induced massive c-Fos expression in the LDT (**Fig. 1a**), the lateral hypothalamic area (LH), the dorsomedial part of the ventromedial hypothalamic nucleus (VMHDM) and the LHb (**Supplementary Fig. 1a–d**). We noted that the olfactory bulb was activated by both TMT and ME, with a greater increase of c-Fos–positive neurons in response to TMT (**Supplementary Fig. 1a**,**d**). Previous studies have shown that the hypothalamus is critical for regulating the autonomic nervous system, including heart rate and hormone release[1,11], as well as being involved in innate defensive behaviors[11–14]. We then focused on the LDT, as no evidence has yet linked this nucleus to fear. We found that the majority of c-Fos–positive neurons in the LDT expressed GAD67, suggesting that they are GABAergic neurons (**Fig. 1a**,**b**).

Next, we determined whether selectively activating GABAergic transmission in the LDT using optogenetics is sufficient to induce fear-like behavior, as judged by four criteria we summarized from previous studies[1,15–17]: defensive behaviors (typically freezing), changing autonomic function such as heart rate and defecation, release of corticosterone, and anxiety-like behavior after prolonged stimulation. In VGAT-ChR2(H134R)-eYFP (abbreviated to VGAT-ChR2)

[1]Department of Neurobiology, Key Laboratory of Medical Neurobiology (Ministry of Health of China), Key Laboratory of Neurobiology of Zhejiang Province, Zhejiang School of Medicine, Hangzhou, China. [2]Department of Neurology, First Affiliated Hospital, Zhejiang University School of Medicine, Hangzhou, China. [3]Key Laboratory of Magnetic Resonance in Biological Systems and State Key Laboratory of Magnetic Resonance and Atomic and Molecular Physics, Wuhan Institute of Physics and Mathematics, CAS Center for Excellence in Brain Science and Intelligence Technology, Chinese Academy of Sciences, Wuhan, China. [4]Wuhan National Laboratory for Optoelectronics, Wuhan, China. [5]These authors contributed equally to this work. Correspondence should be addressed to S.D. (duanshumin@zju.edu.cn) or H.W. (haowang@zju.edu.cn).

Received 30 July 2015; accepted 30 November 2015; published online 4 January 2016; doi:10.1038/nn.4208

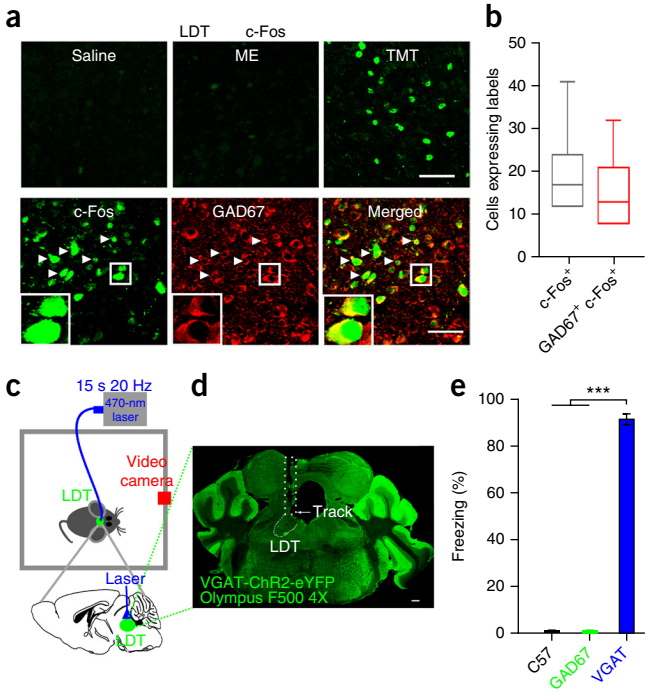

Figure 1 Optogenetic stimulation of GABAergic transmission in the LDT immediately induces freezing behavior in VGAT-ChR2(H134R)-eYFP line BAC transgenic mice. (**a**) Top, representative images of c-Fos expression in the LDT in response to odorant stimuli. Bottom, example images showing that c-Fos–positive neurons (green) in the LDT also expressed GAD67 (red). Scale bars represent 50 μm. (**b**) Quantification of the numbers of cells expressing c-Fos versus GAD67 in the LDT ($n = 12$ slices from 7 mice, $P = 0.413$, $t = 0.848$, unpaired t test). Box limits show first and third quartile, center line is the median and whiskers represent minimum and maximum values. (**c**) Schematic of the light-induced freezing test. (**d**) Example of fiber placement in the LDT. Scale bar represents 250 μm. (**e**) Percentage freezing time during 15 s of light stimulation (20 ms, 20 Hz) in the LDT of WT, GAD67 and VGAT mice ($n = 6$ animals per group, $P < 0.0001$, $F = 1.158 \times 10^{-3}$, one-way ANOVA). ***$P < 0.001$; error bars represent s.e.m.

mice, we observed coexpression of yellow fluorescent protein (YFP) and GAD67 in the LDT (**Supplementary Fig. 2a**). Furthermore, a light stimulus induced action potentials and inward current in YFP-positive neurons in slice preparations (**Supplementary Fig. 2b**). Thus, by using this strain of mice, we were able to effectively and selectively stimulate GABAergic transmission[18] in the LDT.

Previous studies have shown that TMT rapidly induces freezing or hiding behavior in mice, depending on the circumstances[19,20]. Notably, light stimulation of the LDT in VGAT-ChR2 mice also immediately halted their movement. Freezing was maintained during most of the time when the laser was on (**Fig. 1c–e** and **Supplementary Movie 1**). To check that the cessation of movement was not a result of a loss of motor ability, we performed a modified forced-swimming experiment in the presence of light stimulation, and the stimulation failed to stop the mice from swimming (**Supplementary Movie 2**), suggesting that they were able to move during light stimulation. Simultaneous electroencephalogram (EEG) recording during light stimulation ruled out the possibility that the cessation of movement was a result of falling asleep or having a seizure (**Supplementary Fig. 3**). Thus, light stimulation in the LDT of VGAT-ChR2 mice immediately evoked freezing behavior.

Studies in animals and humans have shown that the autonomic nervous system changes rapidly in response to fear[1,2,17,21]. In agreement with previous studies, we found that TMT rapidly accelerated heart rate (**Fig. 2a**) and increased defecation (**Fig. 2b**) in wild-type (WT) mice. Similarly, light stimulation in VGAT-ChR2 mice rapidly increased heart rate (**Fig. 2a**) and enhanced defecation (**Fig. 2b**).

In rodents, the serum corticosterone level is a notable marker that is strongly associated with the stress response[16] and was raised by TMT stimulation (**Fig. 2c**). We found that the serum corticosterone level was also augmented by 10 min of light stimulation of the LDT in VGAT-ChR2 mice (**Fig. 2c**).

To determine whether mice display anxiety-like behaviors after prolonged fear-provoking stimulation, we tested the performance of WT mice in the open field and elevated plus maze tests after a 30-min TMT exposure (**Fig. 2d**). After manipulations, all mice were allowed to rest in their home cage for 20 min before behavioral tests. We found that exposure of WT mice to TMT markedly reduced the total distance and total number of center entries in the open field experiment (**Fig. 2e**), and movement distance and percentage of time in an open arm were reduced (**Fig. 2f**). Similar results were obtained in light-stimulated VGAT-ChR2 mice (**Fig. 2g–i**). Furthermore, we found that VGAT-ChR2 mice showed anxiety-like behaviors even 24 h after 10-min of light stimulation, as indicated by the elevated plus maze and dark-lit box tests (**Supplementary Fig. 4**). These data suggest that prolonged stimulation with TMT exposure and light stimulation are sufficient to induce anxiety-like behavior in WT and VGAT-ChR2 mice, respectively. Taken together, our results demonstrate that optogenetically exciting GABAergic transmission in the LDT is sufficient to induce fear, given that the behavioral changes evoked by light stimulation mimicked those of TMT exposure and satisfied all of the criteria defining fear.

To test whether the fear response was caused by local GABA release in the LDT or by activation of GABAergic outputs to downstream nuclei, we applied GABA receptors antagonists directly into the LDT. We found that local injection of the GABAb receptor antagonist phaclofen (50 ng) into the LDT greatly reduced the freezing responses provoked by TMT (**Fig. 3a,b**). Application of the GABAa receptor antagonist bicuculline at a low dose (10 ng) had no effects on the TMT-induced freezing, but did induce seizure-like behavior at >12.5 ng (data not shown). The LDT contains a mixture of cholinergic, glutamatergic and GABAergic neurons[22]. It is very likely that GABAergic transmission inhibits the principal neurons in the LDT and mediates the fear response. To test this idea, we first injected AAV-CAG-Dio-eArch3.0-eGFP virus (AAV2/9) into the LDT of Thy1-Cre mice. Selective expression of Arch on excitatory neurons in the LDT was observed 4 weeks after injection. We then found that yellow laser stimulation of the LDT produced freezing-like behavior (**Fig. 3c–f**).

PV$^+$ and SOM$^+$ interneurons antagonistically regulate fear

Using immunohistochemical methods, we found that both PV and somatostatin (SOM) were expressed in the LDT (**Fig. 4a**), suggesting the presence of at least two subtypes of interneuron. We then asked which subtypes were involved in light-induced fear. Injection of AAV-CAG-Flex-rev-ChR2(H134R)-mCherry (AAV2/8) virus into the LDT of PV-Cre mice resulted in the expression of ChR2 on PV$^+$ interneurons (PV-ChR2; **Supplementary Fig. 5a–c**), this was confirmed by showing neurons in the LDT that coexpressed ChR2 and PV (**Supplementary Fig. 5d**). Photostimulation of the LDT markedly increased the percentage freezing time in PV-ChR2 mice, but had little effect in PV-GFP control mice (**Fig. 4b**). These results suggest that activation of local PV$^+$ cells in the LDT is sufficient to produce fear-like behavior (**Supplementary Movie 3**). To address whether this behavior was indeed related to innate fear, we determined

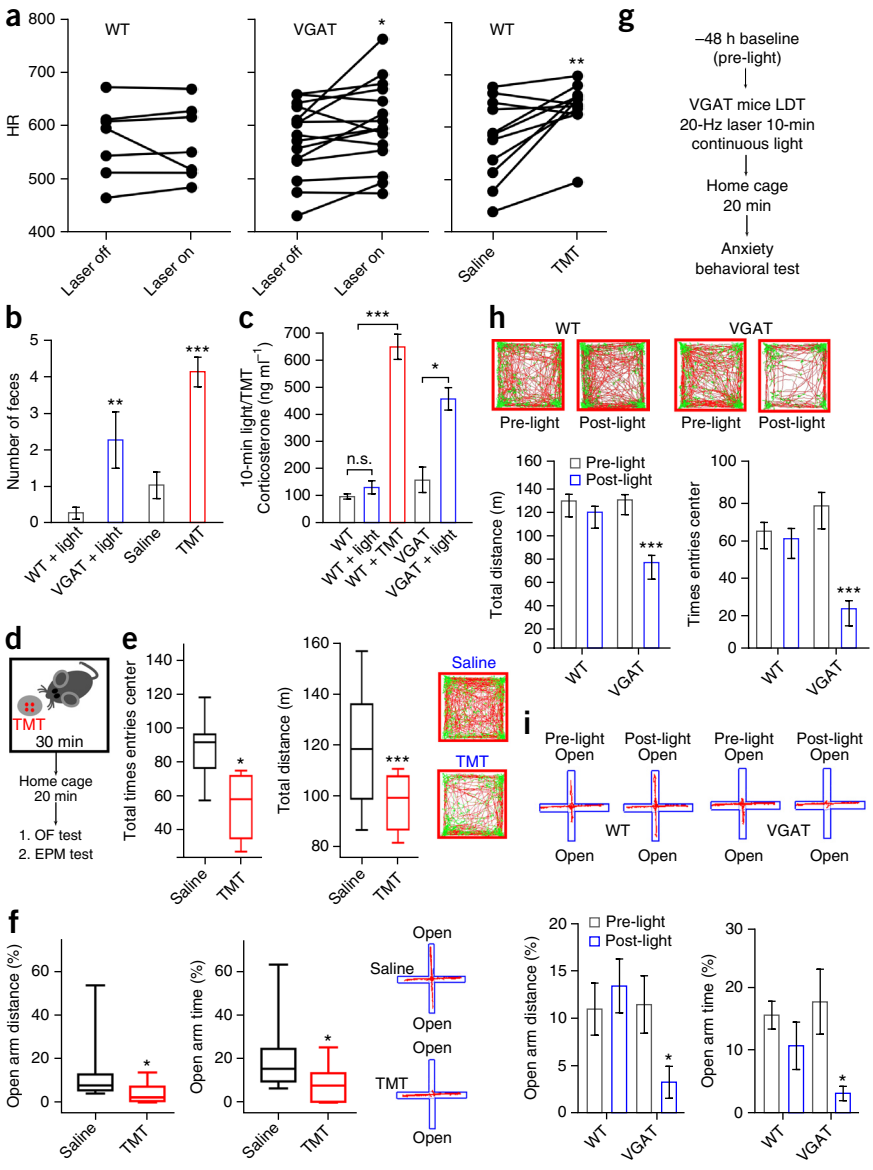

Figure 2 Optogenetic stimulation of GABAergic transmission in the LDT induces anxiety-like responses. (**a**) Heart rate (HR) changes induced by light stimulation and TMT (Light WT: $n = 7$ mice, $P = 0.735$, $t = 0.355$; light VGAT: $n = 15$ mice, $P = 0.04$, $t = 2.262$; TMT: $n = 11$, $P = 0.01$, $t = 3.151$; paired t tests). (**b**) Fecal counts induced by 10 min of light and odorant stimulation (WT-VGAT: $n = 8$ mice, $P = 0.007$, $U = 8.0$; Saline-TMT: $n = 12$ mice, $P < 0.0001$, $U = 3.5$; Mann-Whitney test). (**c**) Serum corticosterone levels in control, TMT-treated and light-stimulated groups (TMT: $n = 8$ mice, $P < 0.0001$, $F = 99.553$; light VGAT: $n = 8$ mice, $P = 0.028$, $F = 6.035$; WT versus WT + light: $n = 8$ mice, $P = 0.245$ (n.s.), $F = 1.471$; one-way ANOVA). (**d**,**g**) Schematic of experimental protocol. OF, open field; EPM, elevated plus maze. (**e**,**h**) Real-time movement traces and behavioral performance in the open field in TMT-exposed or light-stimulated mice, respectively (TMT, center entries times: $n = 10$ mice, $P = 0.035$, $U = 23.0$; distance: $P = 0.001$, $U = 8.0$, Mann-Whitney test; light VGAT, center entries times: $n = 8$ mice, $P = 0.001$, $F = 7.409$; distance: $P < 0.001$, $F = 8.715$, two-way ANOVA). (**f**,**i**) Elevated plus maze movement traces and summary graphs for time spent and distance moved on the open arms in the elevated plus maze for different groups (TMT, distance (%): $n = 10$ mice, $P = 0.035$, $U = 22.0$; time (%): $P = 0.049$, $U = 24.0$, Mann-Whitney test; light VGAT, distance (%): $n = 7$–9 mice, $P = 0.034$, $F = 3.331$; time (%): $P = 0.039$, $F = 3.187$, two-way ANOVA). $^*P < 0.05$, $^{**}P < 0.01$, $^{***}P < 0.001$. In box plots, box limits show first and third quartile, center line is the median and whiskers represent minimum and maximum values. In other data, error bars represent s.e.m.

whether selective suppression of the activity of PV$^+$ cells in the LDT had any effect on TMT-induced fear. Injection of AAV-CAG-Dio-eArch3.0-eGFP virus (AAV2/9) into the LDT of PV-Cre mice resulted in the selective expression of archaerhodopsin (Arch) on PV$^+$ interneurons (PV-Arch; **Supplementary Fig. 6**). Light-driven outward proton pumps mediate the powerful and safe silencing of neuronal activity[23]. We found that yellow light stimulation of the LDT in PV-Arch mice markedly reduced the freezing-time of TMT-induced fear behavior (**Fig. 4c** and **Supplementary Movie 4**), but did not affect the freezing response induced by an auditory cue in mice with previous fear-conditioned learning (**Fig. 4d** and **Supplementary Fig. 7**). Thus, silencing PV$^+$ cells specifically suppresses the innate fear freezing reaction induced by predator odor without apparent effects on the conditioned fear response.

To investigate the role of LDT SOM$^+$ interneurons in fear behavior, we first obtained SOM-ChR2 mice by crossing SOM-Cre mice with Ai32 mice (**Supplementary Fig. 8a**). To our surprise, we found that excitation of SOM$^+$ cells in the LDT not only failed to induce freezing behavior when the laser was on (**Supplementary Fig. 8b**,**c**), but also substantially reduced the freezing time in response to TMT (**Fig. 4e** and **Supplementary Movie 5**). Similar to the effect of light stimulation in PV-Arch mice, such stimulation in SOM-ChR2 mice failed to affect the freezing behavior induced by a conditioned auditory cue (**Fig. 4f** and **Supplementary Fig. 7**).

LHb is upstream of the LDT in innate fear circuit

To identify the upstream nucleus that activates the GABAergic interneurons in the LDT, we first injected the retrograde tracer Fluoro-Gold into the LDT. Many nuclei were retrogradely labeled, but we noted that the LDT received apparent bilateral excitatory inputs from the LHb and hypothalamus (data not shown). Given that the LHb, LH and VMHdm were also specifically activated by TMT (**Supplementary Fig. 1**), we next determined whether LDT interneurons receive direct innervation from these nuclei using a Cre-dependent retrograde trans-synaptic rabies virus[24]. We injected AAV-CAG-Dio-TVA-GFP (AAV2/9) and AAV-CAG-Dio-RG (AAV2/9) on day 1 and EnvA-pseudotyped, glycoprotein(RG)-deleted and DsRed-expressing rabies virus (RV-EvnA-DsRed, RV) on day 21 into the LDT of PV-Cre and SOM-Cre mice (**Fig. 5a–c** and **Supplementary Figs. 9a** and **10a**). On day 28, we observed retrogradely labeled neurons in the bilateral LHb and LH, but not in the VMHdm of both PV-Cre and SOM-Cre mice (**Fig. 5b**,**d** and **Supplementary Figs. 9b** and **10b**), indicating that both interneuron subtypes in the LDT receive monosynaptic bilateral inputs from the LHb and LH. We next focused on the LHb (**Fig. 5e**) and LH and excluded the possibility that the VMHdm is upstream of LDT. It is

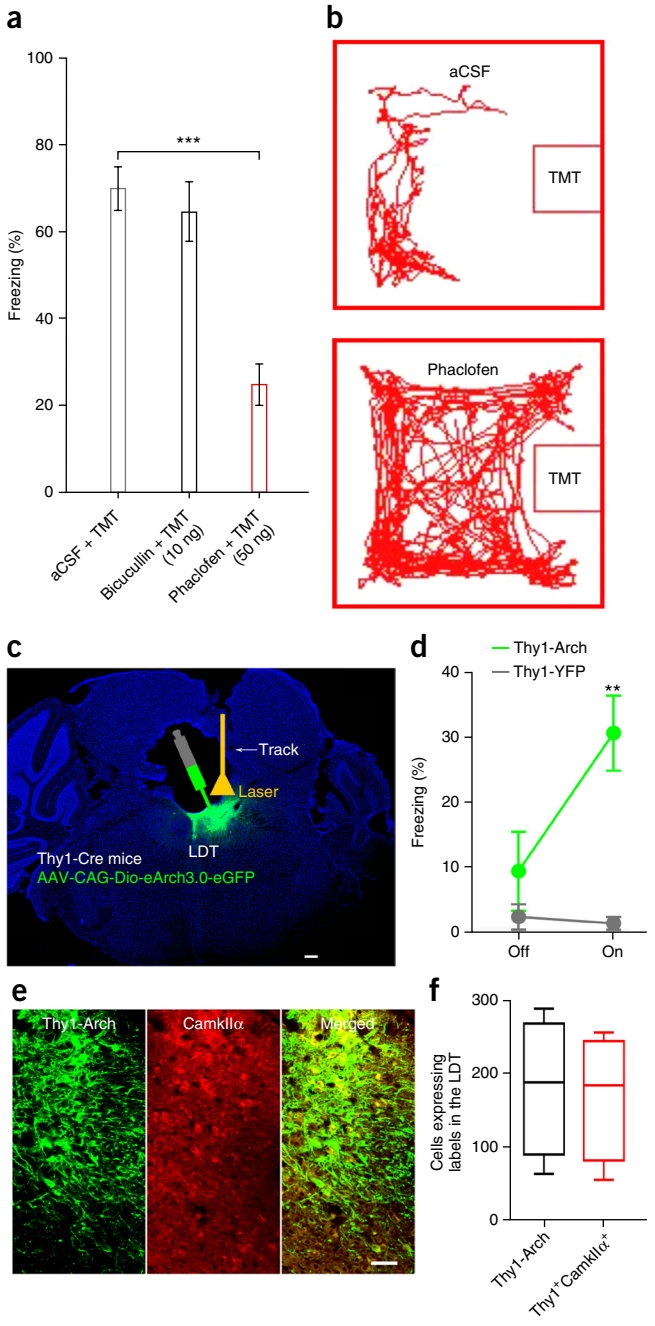

Figure 3 Inhibition of excitatory neurons in the LDT is sufficient to induce fear-like behavior. (**a**) Microinjection of the GABAb receptor antagonist phaclofen (50 ng) greatly reduced the freezing response to TMT (artificial cerebrospinal fluid (aCSF) versus phaclofen: $n = 8$ mice, $P = 0.0001$, $t = 6.517$; aCSF versus bicucullin: $P = 0.545$, $t = 0.620$; unpaired t test). (**b**) Real-time place-preference location plots recorded in response to TMT stimuli for artificial cerebrospinal fluid (top) and phaclofen (bottom) injection groups. (**c**) Example image showing LDT excitatory neurons transfected with Arch-eGFP and the location of the implanted optical fiber. Scale bar represents 200 μm. (**d**) Probability of freezing behavior during 30 s with or without 590-nm light stimulation in the LDT ($n = 5$–8 mice, $P = 0.002$, $F = 6.793$; one-way ANOVA); AAV-EF1a-flex-eYFP–injected mice served as controls. (**e**) Arch-eGFP–labeled neurons were mostly CamkIIα positive. Scale bar represents 50 μm. (**f**) Quantification of GFP and CamkIIα-positive cells in the LDT ($n = 4$ slices) $^{**}P < 0.01$, $^{***}P < 0.001$. In box plots, box limits show first and third quartile, center line is the median and whiskers represent minimum and maximum values. In other data, error bars represent s.e.m.

important to note that a large population of local SOM$^+$ interneurons in the LDT was retrogradely labeled in PV-Cre mice (**Fig. 5c**) and the same situation was observed for PV$^+$ cells, which were also retrogradely labeled in SOM-Cre mice (**Supplementary Fig. 11**). These results indicate that reciprocal synaptic connections exist between SOM$^+$ and PV$^+$ cells in the LTD. Notably, we found the ratio of starter cells to rabies virus–labeled PV$^+$ cells in SOM-Cre mice (115/55) was much higher than that of starter cells to rabies virus–labeled SOM$^+$ cells in PV-Cre mice (18/98; $n = 6$ brain slices), suggesting that PV$^+$ cells received more inputs from SOM$^+$ cells than SOM$^+$ cells did from PV$^+$ cells.

We then transduced the glutamatergic projection neurons in the bilateral LHb with ChR2 by (AAV2/9, CamkIIα-ChR2) virus injection (**Supplementary Fig. 12**) and found nicely labeled terminals around the somata of GAD67-positive neurons in the LDT (**Fig. 5f,g**). Using whole-cell patch recording in slices, we found that light stimulation of LHb terminals in the LDT generated excitatory postsynaptic currents in GABAergic neurons, and these were abolished by application of the AMPA receptor antagonist DNQX (**Fig. 5h,i**). These results suggest that GABAergic neurons in the LDT receive functional glutamatergic inputs from the LHb. We next found that *in vivo* light stimulation of LHb terminals in the LDT rapidly induced freezing behavior (**Fig. 5j** and **Supplementary Movie 6**). Light stimulation time-locked the activity of all ChR2-expressing neurons, and the relevance to stimulation with a natural odor such as TMT was therefore unclear. Combining optogenetics with *in vivo* multiple-electrode recording, we found that the same LDT neuron showed an activity pattern in response to light stimulation of LHb terminals that was similar to that in response to TMT stimulation (**Supplementary Fig. 13**). These results indicate that glutamatergic neurons in the LHb are at least one of the upstream inputs of the LDT in the innate fear pathway. We also injected AAV-CamkIIα-hChR2(H134R)-mCherry (AAV2/9, CamkIIα-hChR2) virus into the LH (**Supplementary Fig. 14a**) and found a large number of virus-labeled terminals in the LDT (**Supplementary Fig. 14b**). We next found that *in vivo* light stimulation of LH excitatory terminals in the LDT rapidly induced standing and stereotyped scratching, which were more likely a stress response, but not typical freezing behaviors (**Supplementary Fig. 14c–g** and **Supplementary Movie 7**). It should be noted that we cannot exclude the possibility that other excitatory inputs drive GABAergic neurons in the LDT and evoke a fear response. For instance, the superior colliculus, periaqueductal gray (PAG) and central amygdala all sent monosynaptic efferents to GABAergic neurons in the LDT (**Supplementary Figs. 9b** and **10b**).

DISCUSSION

Combining *in vivo* optogenetic manipulations, behavioral assays and synaptic electrophysiology, we were able to identify, for the first time to the best of our knowledge, the LDT as the key component in the brain for regulating olfactory cue–induced innate fear (**Supplementary Fig. 15**). With the help of retrograde rabies virus tracing techniques, we found that GABAergic neurons in the LDT received monosynaptic inputs from many innate fear-related nuclei: the prefrontal cortex[25], bed nucleus of the stria terminalis, central amygdaloid nucleus, capsular part[26], basal forebrain[27], PAG, superior colliculus[28,29] and interpeduncular nucleus[30], as well as in the LHb[31] and LH[32] as we reported here (**Supplementary Figs. 9b** and **10b**). These studies indicate that the LDT might be a key node for the innate fear response. In the case of TMT-induced innate fear, we suggest that olfactory information is detected by the olfactory bulb and then transmitted to the LHb via

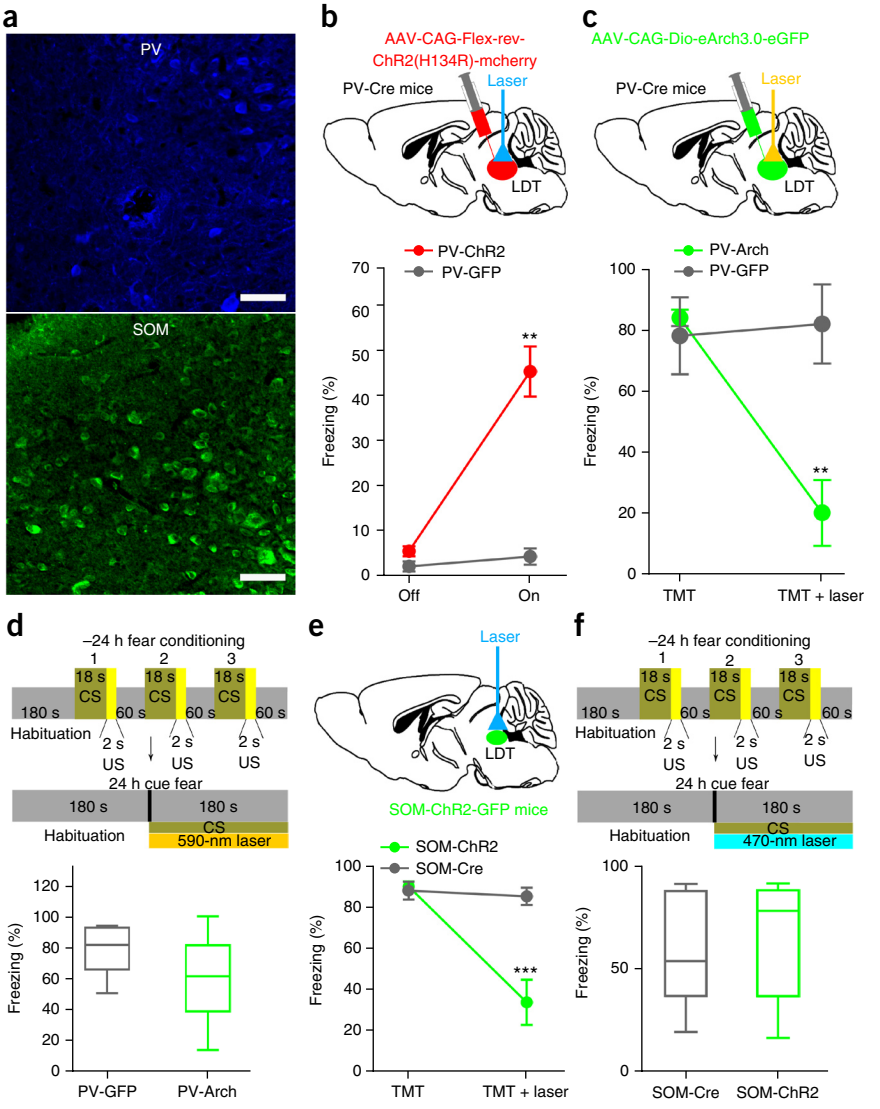

Figure 4 PV+ and SOM+ interneurons in the LDT oppositely regulate innate fear. (**a**) Representative immunostaining images of PV+ (top) and SOM+ (bottom) neurons in the LDT. Scale bars represent 50 μm. (**b**) Top, schematic diagram of LDT injection of AAV-CAG-Flex-rev-ChR2(H134R)-mCherry virus (AAV2/8) in PV-Cre mice. Bottom, summary data showing the percentage of freezing times induced by activation of PV neurons with blue light in the LDT ($n = 8$ mice, $P = 0.002$, $F = 6.418$, two-way ANOVA). (**c**) Top, schematic diagram of LDT injection of AAV-CAG-Dio-eArch3.0-eGFP (AAV2/9) virus in PV-Cre mice or PV-GFP mice. Bottom, summary data showing that inhibition of PV+ interneurons by yellow light markedly reduced the TMT-induced freezing responses ($n = 5$–8 mice, $P = 0.002$, $F = 7.132$, two-way ANOVA). (**d**) Top, schematic of conditioned fear training and the auditory cue–induced fear test. Bottom, summary data for auditory cue–induced freezing responses with light-induced inhibition of PV neurons in the LDT of PV-Arch mice (PV-GFP mice served as control; $n = 5$–8 mice, $P = 0.586$, $t = 0.572$; unpaired t test). (**e**) Top, schematic diagram of the implanted LDT optical fiber in SOM-ChR2 mice. Bottom, light activation of SOM+ interneurons in the LDT markedly reduced the TMT-induced freezing responses (SOM-Cre served as control; $n = 7$ mice, $P < 0.0001$, $F = 8.793$; two-way ANOVA). (**f**) Auditory cue-induced freezing responses with (SOM-ChR2) or without (SOM-Cre) light-induced inhibition of SOM+ interneurons in the LDT ($n = 10$ mice, $P = 0.703$, $t = 0.387$; unpaired t test). $^{**}P < 0.01$, $^{***}P < 0.001$. In box plots, box limits show first and third quartile, center line is the median and whiskers represent minimum and maximum values. In other data, error bars represent s.e.m.

polysynaptic connections[33], as no evidence of direct projections from the bulb to the LHb has yet been found. Activation of GABAergic interneurons by glutamatergic inputs from the LHb may sequentially regulate the activity of cholinergic and glutamatergic neurons in the LDT. Inhibition of excitatory neurons in the LDT may produce freezing-like behaviors either through basal ganglia circuitry such as ventral tegmental area (VTA) or via reverse activation of RMTg to inhibit motor responses[34,35], as well as through two innate fear–related downstream nuclei: the lateral hypothalamus and the dorsomedial part of the ventromedial hypothalamic nucleus[11,32,36,37]. The LDT can regulate heart rate, serum corticosterone levels and anxiety-like behaviors via cholinergic projections to the paraventricular nucleus in the hypothalamus and/or the basal forebrain[16,32,38,39]. In addition, monoaminergic neurons in the locus coeruleus may also be involved in the changes in the autonomic nervous system. Notably, we found that the VTA was not activated by TMT stimulation (**Supplementary Fig. 1d**) and excitation of glutamatergic inputs from the LDT to the VTA induced strong conditioned place preference (data not shown), consistent with previous studies[40]. These results indicate that the LDT regulates multiple emotional responses through different downstream pathways. That is, the LDT has a key role in controlling innate behaviors including both reward and aversion.

To our surprise, we found that exciting PV+ and SOM+ interneurons had different effects on innate fear–like behavior. A possible explanation for their distinct roles could be that SOM+ interneurons interact not only with principal neurons, but also with PV+ interneurons. Our results suggest that, although inhibition of glutamatergic neurons in the LDT by PV+ cells evoke freezing, activation of SOM+ cells reduces freezing through disinhibition of PV+ cells. This speculation is supported by recent studies in the amygdale[41]. We found that PV+ and SOM+ cells in the LDT were reciprocally synaptic connected (**Fig. 5c** and **Supplementary Fig. 11**), with denser innervations from SOM+ to PV+ cells. Direct inhibition of PV+ cells by SOM+ cells may be responsible for reducing freezing responses induced by activation of SOM+ cells. Apparently, the distinct upstream and downstream pathways of two types interneuron should be critical for the opposite effects of SOM+ and PV+ cells in regulating freezing behavior. The differential modulation of PV+ and SOM+ interneurons may permit flexible regulation of behaviors, such as the freezing or hiding response to a predator. In addition, we found that exciting PV+ neurons in the LDT alone recaptured the freezing-like changes induced by activation of glutamatergic inputs from the LHb or photostimulation in VGAT-ChR2 mice, whereas selective activation of SOM+ cells in the LDT had an opposite effect on innate fear responses. It is possible that, in the former two cases, SOM+ cells in the LDT may not be effectively activated by glutamatergic inputs from LHb or by direct photostimulation of LDT in VGAT-ChR2 mice due to a strong feedforward or light-induced inhibition from PV+ to SOM+

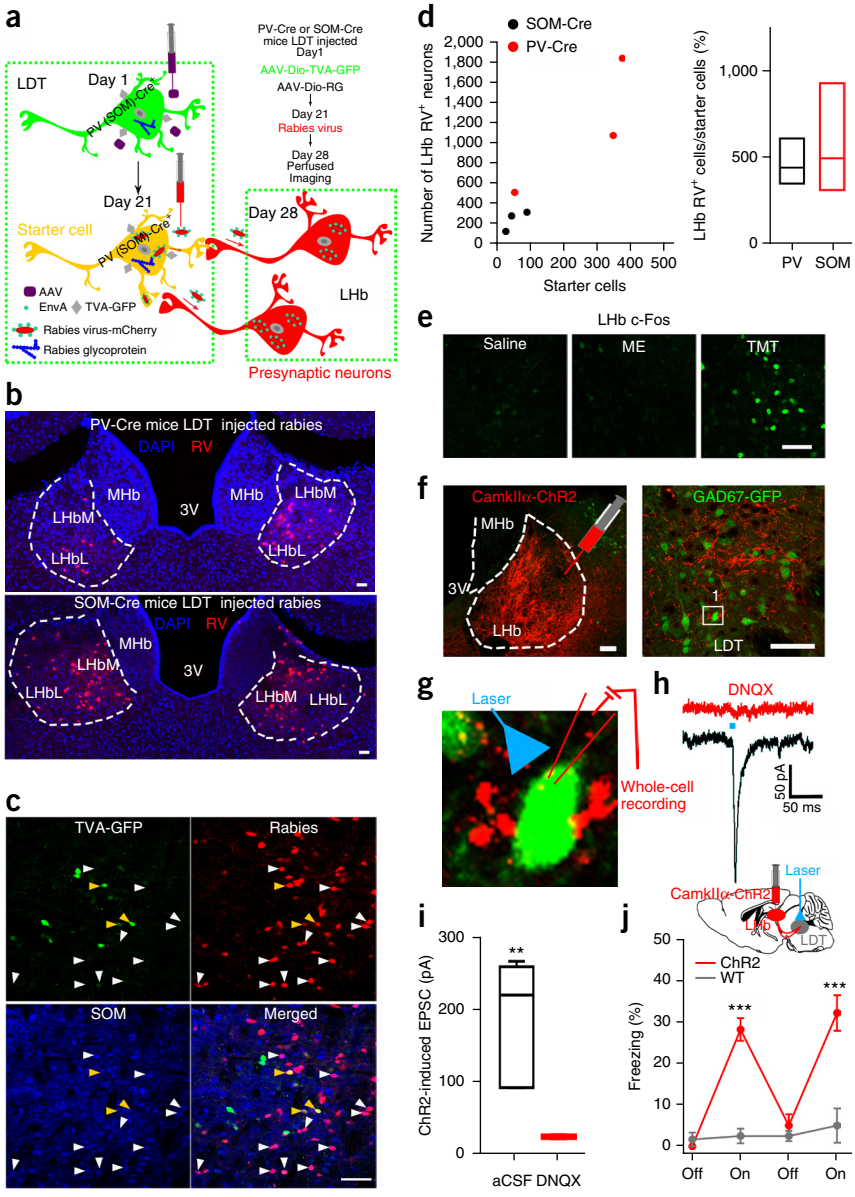

Figure 5 Activation of LDT interneurons by LHb glutamatergic inputs is sufficient to induce fear-like behavior. (**a**) Schematic diagram of LDT injection of AAV-CAG-Dio-TVA-eGFP (AAV2/9) virus and AAV-CAG-Dio-RG (AAV2/9) on day 1 and RV-EvnA-DsRed on day 21 in SOM-Cre or PV-Cre mice to retrogradely trace the input neurons (red) to LDT interneurons (yellow, starter neurons). (**b**) Typical examples of DsRed-expressing LHb neurons retrogradely labeled by LDT injection of virus in PV-Cre (top) and SOM-Cre (bottom) mice. Both interneuron subtypes received bilateral LHb projections. Scale bars represent 50 μm. (**c**) Example images of the LDT from PV-Cre mice showing that PV$^+$ interneurons (green) also received local monosynaptic inputs from SOM$^+$ interneurons (blue). Yellow arrowheads, starter neurons (infected by both TVA-eGFP and rabies virus); white arrowheads, retrogradely traced SOM neurons (transfected with rabies virus only). Scale bar represents 50 μm. (**d**) Quantification of RV-labeled cells in the LHb retrogradely from PV$^+$ or SOM$^+$ interneurons in the LDT ($n = 3$ mice, $P = 0.603$, $F = 0.319$; one-way ANOVA). (**e**) Representative images of c-Fos expression patterns in the LHb of mice with different treatments. Scale bar represents 50 μm. (**f**) Left, example image of LHb neurons transfected with AAV-CamkIIα-hChR2(H134R)-mCherry (AAV2/9, CamkIIα-ChR2) with locally injected virus. Scale bar represents 40 μm. Right, example image of LDT slice from a GAD67-GFP mouse with LHb injection of CamkIIα-ChR2 virus showing the distribution of CamkIIα-ChR2-positive terminals (red) surrounding GABAergic neurons (green). Scale bars represent 50 μm. (**g**) Enlarged image of the boxed area in the right image in **f**. (**h**) Example excitatory postsynaptic currents (EPSCs) recorded in an LDT GABAergic neuron evoked by light stimulation of CamkIIα-ChR2–positive terminals (lower trace); this was blocked by the non-NMDA receptor antagonist DNQX (upper trace). (**i**) Summary of light-induced EPSCs and their blockade by DNQX ($n = 4$–6 cells from 2 mice, $P = 0.0036$, $t = 4.068$). (**j**) Top, schematic diagram showing injection of CamkIIα-ChR2 virus to transfect LHb glutamatergic neurons and light stimulation of their projection terminals in the LDT to induce behavioral responses. Bottom, probability of freezing behavior during 15 s with or without light stimulation (15 ms, 20 Hz) in the LDT ($n = 8$ mice; ChR2-WT: $P < 0.0001$, $F = 52.905$; ChR2 off on: $P < 0.0001$, $F = 16.0$; repeated ANOVA); injection of AAV-EF1a-flex-eYFP (AAV2/9) in the LHb as controls. $^{**}P < 0.01$, $^{***}P < 0.001$. In box plots, box limits show first and third quartile, center line is the median and whiskers represent minimum and maximum values. In other data, error bars represent s.e.m.

cells. Thus, the reciprocal synaptic connections between two populations of interneuron constitute a very efficient mechanism for the bi-directional regulation of freezing responses.

Consistent with our pharmacological studies indicating that GABAb receptors were involved in fear response (**Fig. 3**), we found that they were abundantly expressed in the CamkIIα-positive projection cells in the LDT (data not shown). These results suggest that GABAb receptors in the LDT may be involved in fear regulation. It is important to note that, although our data support the idea that a local inhibition of principal neurons through GABAergic transmission in the LDT causes a fear response, we cannot exclude the possibility of excitation of efferent PV$^+$ cells. Indeed, we found that PV$^+$ cells in the LDT also projected to the dorsal raphe nucleus interfascicular, locus coeruleus and medial parabrachial nucleus (**Supplementary Fig. 6b**). Notably, the latter two nuclei may mediate the fear response[42,43].

Although GABAergic neurons in the LDT receive excitatory inputs from LH, the role of LH in innate fear is not clear, as activation of LH-LDT pathway cannot induce typical freezing response. It is possible that LH regulates other aspects of fear response, such as stress. This hypothesis was supported by the fact that the activation of LH-LDT pathway induced standing and stereotyped scratching behaviors (**Supplementary Movie 7**), which might be related to stress. In addition, studies have shown that LH is involved in mediating stress-like behaviors[32]. Alternatively, instead of being upstream of the LDT, LH may function downstream of the LDT in the innate fear pathway, as the LDT also sends excitatory projections to the LH[37]. Further studies are needed to elucidate the whole picture of pathways mediating olfactory cue–induced innate fear.

The LHb has recently been reported to be important in depression[44,45]. These findings raise the question of whether the LHb regulates depressive behavior through its output to the LDT. The LDT has been identified as

a rapid eye-movement–on region[46]. It is well-known that anxious and depressed patients tend to have sleep disorders, especially with regard to rapid eye-movement episodes[47,48]. Besides, most of the anxiety-related changes, including hormonal changes, physiological manifestations and behavioral alteration, occurred during or after the activation of GABAergic transmission in the LDT, indicating its potential role in anxiety. Our findings provide a neuronal link for the pathology of abnormal innate fear and its related diseases, such as anxiety disorder.

METHODS

Methods and any associated references are available in the online version of the paper.

Note: Any Supplementary Information and Source Data files are available in the online version of the paper.

ACKNOWLEDGMENTS

We thank G. Feng (Massachusetts Institute of Technology) for providing the VGAT-ChR2 (H134R)-eYFP mice and X. Zhang (Beijing Normal University) for providing the PV-Cre and SOM-Cre mice. We also thank I.C. Bruce for critically reading the paper. This work was supported by grants from the Major State Basic Research Program of China (2011CB504400, 2013CB945600 and 2015AA020515), the National Natural Science Foundation of China (31190060, 31471022, 31490590, 91232000, 91132307, 81221003 and 31471308), the National Key Technology R&D Program of the Ministry of Science and Technology of China (2012BAI01B08), the Program for Introducing Talents in Disciplines to Universities, the Zhejiang Provincial Natural Science Foundation of China (Y2110057) and Fundamental Research Funds for the Central Universities (2014FZA7007).

AUTHOR CONTRIBUTIONS

H.Y., S.D. and H.W. designed the project, and H.Y. and J.Y. performed virus or drug injections, optogenetic behavior, electrophysiology experiments, and collected and analyzed the data. W.X. and S.H. helped to collect the data. H.Y. and S.H. performed immunohistochemistry and quantitatively analyzed the imaging data. W.X. designed the micro drive optrode system and performed freely moving recording. X.H. generated rabies and pseudo-rabies virus and F.X. supervised retrograde virus labeling experiments. B.L., H.L., L.Z., H.Y., Y.Y., S.D. and H.W. interpreted the results and commented on the manuscript. H.W. and S.D. wrote the manuscript. H.W. supervised all aspects of the project.

COMPETING FINANCIAL INTERESTS

The authors declare no competing financial interests.

1. Blanchard, D.C. & Blanchard, R.J. Ethoexperimental approaches to the biology of emotion. *Annu. Rev. Psychol.* **39**, 43–68 (1988).
2. Ohman, A. & Mineka, S. Fears, phobias, and preparedness: toward an evolved module of fear and fear learning. *Psychol. Rev.* **108**, 483–522 (2001).
3. Battaglia, M. & Ogliari, A. Anxiety and panic: from human studies to animal research and back. *Neurosci. Biobehav. Rev.* **29**, 169–179 (2005).
4. Knapska, E. *et al.* Functional anatomy of neural circuits regulating fear and extinction. *Proc. Natl. Acad. Sci. USA* **109**, 17093–17098 (2012).
5. Sotres-Bayon, F., Sierra-Mercado, D., Pardilla-Delgado, E. & Quirk, G.J. Gating of fear in prelimbic cortex by hippocampal and amygdala inputs. *Neuron* **76**, 804–812 (2012).
6. Maren, S., Phan, K.L. & Liberzon, I. The contextual brain: implications for fear conditioning, extinction and psychopathology. *Nat. Rev. Neurosci.* **14**, 417–428 (2013).
7. Rosen, J.B. The neurobiology of conditioned and unconditioned fear: a neurobehavioral system analysis of the amygdala. *Behav. Cogn. Neurosci. Rev.* **3**, 23–41 (2004).
8. Wallace, K.J. & Rosen, J.B. Neurotoxic lesions of the lateral nucleus of the amygdala decrease conditioned fear but not unconditioned fear of a predator odor: comparison with electrolytic lesions. *J. Neurosci.* **21**, 3619–3627 (2001).
9. Root, C.M., Denny, C.A., Hen, R. & Axel, R. The participation of cortical amygdala in innate, odour-driven behaviour. *Nature* **515**, 269–273 (2014).
10. Dielenberg, R.A., Hunt, G.E. & McGregor, I.S. "When a rat smells a cat": the distribution of Fos immunoreactivity in rat brain following exposure to a predatory odor. *Neuroscience* **104**, 1085–1097 (2001).
11. Wang, L., Chen, I.Z. & Lin, D. Collateral pathways from the ventromedial hypothalamus mediate defensive behaviors. *Neuron* **85**, 1344–1358 (2015).
12. Lee, H. *et al.* Scalable control of mounting and attack by Esr1+ neurons in the ventromedial hypothalamus. *Nature* **509**, 627–632 (2014).
13. Lin, D. *et al.* Functional identification of an aggression locus in the mouse hypothalamus. *Nature* **470**, 221–226 (2011).
14. Gross, C.T. & Canteras, N.S. The many paths to fear. *Nat. Rev. Neurosci.* **13**, 651–658 (2012).
15. Fendt, M., Endres, T., Lowry, C.A., Apfelbach, R. & McGregor, I.S. TMT-induced autonomic and behavioral changes and the neural basis of its processing. *Neurosci. Biobehav. Rev.* **29**, 1145–1156 (2005).
16. Tovote, P. *et al.* Heart rate dynamics and behavioral responses during acute emotional challenge in corticotropin-releasing factor receptor 1-deficient and corticotropin-releasing factor-overexpressing mice. *Neuroscience* **134**, 1113–1122 (2005).
17. Ekman, P., Levenson, R.W. & Friesen, W.V. Autonomic nervous system activity distinguishes among emotions. *Science* **221**, 1208–1210 (1983).
18. Zhao, S. *et al.* Cell type–specific channelrhodopsin-2 transgenic mice for optogenetic dissection of neural circuitry function. *Nat. Methods* **8**, 745–752 (2011).
19. Takahashi, L.K., Nakashima, B.R., Hong, H. & Watanabe, K. The smell of danger: a behavioral and neural analysis of predator odor-induced fear. *Neurosci. Biobehav. Rev.* **29**, 1157–1167 (2005).
20. Wallace, K.J. & Rosen, J.B. Predator odor as an unconditioned fear stimulus in rats: elicitation of freezing by trimethylthiazoline, a component of fox feces. *Behav. Neurosci.* **114**, 912–922 (2000).
21. Nestler, E.J. *et al.* Neurobiology of depression. *Neuron* **34**, 13–25 (2002).
22. Wang, H.L. & Morales, M. Pedunculopontine and laterodorsal tegmental nuclei contain distinct populations of cholinergic, glutamatergic and GABAergic neurons in the rat. *Eur. J. Neurosci.* **29**, 340–358 (2009).
23. Chow, B.Y. *et al.* High-performance genetically targetable optical neural silencing by light-driven proton pumps. *Nature* **463**, 98–102 (2010).
24. Wickersham, I.R. *et al.* Monosynaptic restriction of transsynaptic tracing from single, genetically targeted neurons. *Neuron* **53**, 639–647 (2007).
25. Likhtik, E., Stujenske, J.M., Topiwala, M.A., Harris, A.Z. & Gordon, J.A. Prefrontal entrainment of amygdala activity signals safety in learned fear and innate anxiety. *Nat. Neurosci.* **17**, 106–113 (2014).
26. Sharma, A., Rale, A., Utturwar, K., Ghose, A. & Subhedar, N. Identification of the CART neuropeptide circuitry processing TMT-induced predator stress. *Psychoneuroendocrinology* **50**, 194–208 (2014).
27. Janitzky, K. *et al.* Behavioral effects and pattern of brain c-fos mRNA induced by 2,5-dihydro-2,4,5-trimethylthiazoline, a component of fox feces odor in GAD67-GFP knock-in C57BL/6 mice. *Behav. Brain Res.* **202**, 218–224 (2009).
28. Kessler, M.S. *et al.* fMRI fingerprint of unconditioned fear-like behavior in rats exposed to trimethylthiazoline. *Eur. Neuropsychopharmacol.* **22**, 222–230 (2012).
29. Wei, P. *et al.* Processing of visually evoked innate fear by a non-canonical thalamic pathway. *Nat. Commun.* **6**, 6756 (2015).
30. Yamaguchi, T., Danjo, T., Pastan, I., Hikida, T. & Nakanishi, S. Distinct roles of segregated transmission of the septo-habenular pathway in anxiety and fear. *Neuron* **78**, 537–544 (2013).
31. Pobbe, R.L. & Zangrossi, H. Jr. Involvement of the lateral habenula in the regulation of generalized anxiety- and panic-related defensive responses in rats. *Life Sci.* **82**, 1256–1261 (2008).
32. Sokolowski, K. *et al.* Specification of select hypothalamic circuits and innate behaviors by the embryonic patterning gene dbx1. *Neuron* **86**, 403–416 (2015).
33. Pérez-Gómez, A. *et al.* Innate predator odor aversion driven by parallel olfactory subsystems that converge in the ventromedial hypothalamus. *Curr. Biol.* **25**, 1340–1346 (2015).
34. Lenard, L.G. & Beer, B. 6-Hydroxydopamine and avoidance: possible role of response suppression. *Pharmacol. Biochem. Behav.* **3**, 873–878 (1975).
35. Jhou, T.C., Fields, H.L., Baxter, M.G., Saper, C.B. & Holland, P.C. The rostromedial tegmental nucleus (RMTg), a GABAergic afferent to midbrain dopamine neurons, encodes aversive stimuli and inhibits motor responses. *Neuron* **61**, 786–800 (2009).
36. Kunwar, P.S. *et al.* Ventromedial hypothalamic neurons control a defensive emotion state. *eLife* **4**, e06633 (2015).
37. Cornwall, J., Cooper, J.D. & Phillipson, O.T. Afferent and efferent connections of the laterodorsal tegmental nucleus in the rat. *Brain Res. Bull.* **25**, 271–284 (1990).
38. Berntson, G.G., Sarter, M. & Cacioppo, J.T. Anxiety and cardiovascular reactivity: the basal forebrain cholinergic link. *Behav. Brain Res.* **94**, 225–248 (1998).
39. Palkovits, M. Interconnections between the neuroendocrine hypothalamus and the central autonomic system. Geoffrey Harris Memorial Lecture, Kitakyushu, Japan, October 1998. *Front. Neuroendocrinol.* **20**, 270–295 (1999).
40. Lammel, S. *et al.* Input-specific control of reward and aversion in the ventral tegmental area. *Nature* **491**, 212–217 (2012).
41. Wolff, S.B. *et al.* Amygdala interneuron subtypes control fear learning through disinhibition. *Nature* **509**, 453–458 (2014).
42. Balaban, C.D. & Thayer, J.F. Neurological bases for balance-anxiety links. *J. Anxiety Disord.* **15**, 53–79 (2001).
43. Carter, M.E. *et al.* Tuning arousal with optogenetic modulation of locus coeruleus neurons. *Nat. Neurosci.* **13**, 1526–1533 (2010).
44. Li, K. *et al.* βCaMKII in lateral habenula mediates core symptoms of depression. *Science* **341**, 1016–1020 (2013).
45. Li, B. *et al.* Synaptic potentiation onto habenula neurons in the learned helplessness model of depression. *Nature* **470**, 535–539 (2011).
46. Boucetta, S., Cissé, Y., Mainville, L., Morales, M. & Jones, B.E. Discharge profiles across the sleep-waking cycle of identified cholinergic, GABAergic, and glutamatergic neurons in the pontomesencephalic tegmentum of the rat. *J. Neurosci.* **34**, 4708–4727 (2014).
47. Benca, R.M., Obermeyer, W.H., Thisted, R.A. & Gillin, J.C. Sleep and psychiatric disorders. A meta-analysis. *Arch. Gen. Psychiatry* **49**, 651–668, discussion 669–670 (1992).
48. Goldstein, A.N. & Walker, M.P. The role of sleep in emotional brain function. *Annu. Rev. Clin. Psychol.* **10**, 679–708 (2014).

ONLINE METHODS

Animals. In all experiments, VGAT-ChR2(H134R)-eYFP (VGAT), GAD67-GFP (GAD67), PV-Cre, PV-GFP, SOM-Cre, Thy1-Cre, Ai32, Ai47 and C57BL/6J male mice were used. Mice at 2–4 months of age were singly housed 2 weeks before experiments, under 22 ± 1 °C and 55 ± 5% humidity with food and water *ad libitum*. Animal experiments were conducted in accordance with the Guidelines for the Care and Use of Laboratory Animals of Zhejiang University.

Virus injection. AAV-CamkIIα-hChR2(H134R)-mCherry (AAV2/9, 1.97×10^{13} genomic copies per ml), AAV-CAG-Flex-rev-ChR2(H134R)-mCherry (AAV2/8, 1.25×10^{12} genomic copies per ml), AAV-EF1a-flex-eYFP (AAV2/9, 1.0×10^{12} genomic copies per ml), and AAV-CAG-Dio-eArch3.0-eGFP (AAV2/9, 2.71×10^{12} genomic copies per ml) were made by NeuronBiotech or Hanbio. AAV-CAG-Dio-TVA-eGFP (AAV2/9, 1.7×10^{13} genomic copies per ml), AAV-CAG-Dio-RG (AAV2/9, 6.8×10^{12} genomic copies per ml), and EnvA-pseudotyped, glycoprotein(RG)-deleted and DsRed-expressing rabies virus (RV-EvnA-DsRed, RV) (5.0×10^{8} genomic copies per ml) were provided by F. Xu (Wuhan, China). GAD67 and PV mice were anesthetized with sodium pentobarbital (1% wt/vol) bilateral for stereotaxic injection of AAV-CaMKIIa-hChR2(H134R)-mCherry into the LHb (AP, −1.8 mm from bregma; ML, ±0.3 mm; DV, −2.5 mm) or unilateral injection of AAV-CAG-Flex-rev-ChR2(H134R)-mCherry/AAV-CAG-Dio-eArch3.0-eGFP into the right-lateral LDT (AP, −5.2 mm from bregma; ML, −0.4 mm; DV, −3.5 mm). We injected 0.3–0.5 µl of virus into each location at 0.05 µl min^{-1}. The syringe was not removed until 15–20 min after the end of infusion to allow diffusion of the virus. After injection, mice were allowed 4–6 weeks of recovery. In monosynaptic tracing experiments, PV-Cre and SOM-Cre mice were microinjected in the LDT with 80 nl viral cocktail (1:1) with AAV-CAG-Dio-TVA-eGFP to allow the initial infection of LDT starter neurons. AAV-CAG-Dio-RG coding for the rabies virus envelope glycoprotein was also injected into the right LDT at the same time to allow the trans-synaptic spread of virus. 3 weeks later, the same location was microinjected with 200 nl of the modified rabies virus. 1 week after the last injection, mice were killed and brain sections were collected for confocal imaging.

Tracer injection. Mice were anesthetized with sodium pentobarbital (1%) before stereotaxic injection into the right LDT of 20 nl Fluoro-Gold (2% in 0.9% NaCl (wt/vol); Fluorochrome) as a retrograde tracer (AP, −5.2 mm; ML, −0.4 mm; DV, −3.5 mm). After injection, the syringe was kept in place for 30 min before removal. 48 hours later, the mice were perfused with phosphate-buffered saline followed by 4% paraformaldehyde (wt/vol) in 0.1 M phosphate buffer. The brain was then removed and placed in 4% paraformaldehyde buffer at 4 °C for overnight fixation. After fixation, the brain was cryoprotected in 30% sucrose (wt/vol) at 4 °C. Coronal sections were cut at 40 µm on a cryostat (Leica CM1900) for imaging.

Cannula implants and *in vivo* optogenetic manipulation. For *in vivo* optogenetic manipulation in awaked behaving animals, an optical fiber cannula (diameter, 200 µm RWD Life Science) was implanted into the right LDT (AP, −5.2 mm; ML, −0.4 mm; DV, −3.3 mm). The optic fiber (diameter, 100 µm; Shenzhen Huaying) was connected to a laser source using an optic fiber sleeve. Mice performed behavioral tests after habituation. The power of the blue (470 nm) or yellow laser (590 nm) was 0.83–3.33 mW mm^{-2} as measured at the tip of the optic fiber. The freezing level was calculated as the percentage freezing time during 15 s or 30 s of direct light stimulation in the LDT. Mice with missed injections or cannula locations were excluded. Control group mice underwent the same procedure and received the same intensity of laser stimulation.

EEG and electromyogram (EMG) recording. Mice were anesthetized with sodium pentobarbital (1%) for stereotaxic surgery. A cannula was implanted into the LDT and fixed to the skull with dental cement. Another three small holes were drilled into the skull for recording electrodes in the prefrontal cortex, parietal cortex and ground to record EEG. For EMG recording, the left and right nuchal muscles were exposed and Teflon-coated stainless-steel electrodes were sutured to each muscle. Finally, the cannula, wires, screws and assembly were fixed to the skull with dental cement. After 5–8 d of recovery, a light-weight cable was connected to the assembly on the head. Cortical EEG was filtered at 0.5–100 Hz or 50–300 Hz and neck EMG was filtered at 100–1,000 Hz.

Anxiety-like behavioral test. The open field, elevated plus maze and light-dark box tests were carried out after 30-min exposure to TMT or 10-min continuous blue light stimulation in the LDT (C57 mice as controls) (20 ms, 20 Hz, 3.3 mW). In the open field test, mice reduce their spontaneous activity when continuously tested in the same test arena. To avoid this, we collected the baseline data 2 d ahead of experiments during habitation.

Open field test. The open field test was used to assess anxiety-related behavior and locomotor activity in an open field arena (50 cm long, 50 cm wide and 60 cm high). Experiments were conducted under low light conditions in order to minimize anxiety effects. The distance traveled and the number of center entries was recorded for 30 min using MED behavioral analysis software. The area was cleaned with 75% ethanol between tests.

Elevated plus-maze test. The elevated plus-maze consisted of a plus-shaped platform with four intersecting arms: two opposing open arms and two closed arms. Animals were placed in the center of the apparatus facing a closed arm and allowed to freely explore the maze for 5 min. The parameters open arm time and open arm distance traveled were analyzed with the MED software. The area was cleaned with 75% ethanol between tests.

Light-dark box test. The light-dark box consisted of one dark compartment and one brightly lit compartment. The light-dark box test was usually used to assess anxiety-related behavior. At the beginning of the experiments, mice were placed in the dark compartment facing the lit compartment. During the 5-min test, the time spent in the lit compartment and the number of entries into the lit compartment were assessed using the MED software. The area was cleaned with 75% ethanol between tests.

Feces evaluation. Feces were counted during 10 min in mice either under blue light stimulation in the LDT (20 Hz, 15 s per min) or exposed to TMT. The experimental box was cleaned with 75% ethanol for each test.

Electrocardiogram (ECG) recording and heart rate analysis. Mice were separated and housed singly 2 weeks before the experiment, with handling twice every day. Experiments were performed in the morning (09:30–10:30). Heart rate was evaluated using a non-invasive blood-pressure test system (Gene & I, BP-98A) either after 3–5-min exposure to TMT or during light-induced freezing. Briefly, each mouse was held in a mouse-bag and an arterial pulse sensor was fixed to the tail. After habituation for 3–5 min, ECG was simultaneously collected while blue light was applied to the LDT or during TMT exposure. Heart rate was analyzed with the ECG recording software. Each mouse was tested five times, and the mean heart rate was calculated.

Hormone measurements. To determine the basal hormone plasma levels, mice were housed in an undisturbed environment throughout the night before experiments. Blood sampling was performed in the morning (09:30–10:30) by rapidly collecting trunk blood after decapitation. The time from first handling of the animal to the completion of sampling did not exceed 20 s. We collected blood samples after 3 min of TMT exposure or 10 min of light stimulation in the LDT (20 Hz, 15 s per min). Blood samples were centrifuged at 1,000 *g* for 20 min at 4 °C. Supernatant was collected and plasma corticosterone concentrations were measured in duplicates using commercially-available ELISA kits (Enzo ADI-900-097).

Fear conditioning. For auditory fear conditional training, mice were placed in the conditioning chamber (MED). After habituation for 180 s, a pure tone (80 dB, 9 kHz) was presented for 20 s (conditioned stimulus, CS) that co-terminated with a 2-s footshock (unconditioned stimulus, US) of 0.75 mA. Another two similar CS + US pairs were delivered at intervals of 60 s. After the last training, animals remained in the shock context for an additional 60 s before being returned to their home cages. 24 h later, bedding (wood shavings) was placed underneath the grid and a triangular plate was used to change the chamber wall. Mice were placed in the new chamber and adapted for 180 s, then the CS was presented for 180 s with 20-Hz continuous 470-nm blue laser stimulation to SOM-ChR2 mice (SOM-Cre mice as control) or continuous 590-nm yellow laser stimulation to PV-arch mice (PV-GFP mice as control). The cue-induced freezing was calculated with the MED software.

doi:10.1038/nn.4208

Freezing level of innate fear. Mice were directly placed in an organic glass box with a TMT odor dish in one corner. 30-s cycles of blue or yellow light were delivered to the LDT while the mice were immobile. The percentage freezing time was calculated for each 30-s stimulus, and the values for all stimulations were averaged to give the freezing level for each mouse. SOM-Cre and PV-GFP mice served as controls.

For the laser-induced freezing behavior experiments, 15-s cycles of blue light were directly delivered into the LDT while the mice were active and then the immobile time induced by the laser was measured by analyzing the video. We used the average of six stimulations as the freezing level. GAD67 and C57 mice were used as controls for VGAT mice. Injection of AAV-CAG-Flex-rev-ChR2(H134R)-mCherry into the LDT of PV-GFP mice was used as control the for PV-ChR2 mice. LHb injection of AAV-EF1a-flex-eYFP mice was used as the control for LHb-CamkIIa-ChR2 mice.

After the behavioral tests, mice were deeply anesthetized with chloral hydrate (10% wt/vol) and perfused with phosphate-buffered saline followed by 4% paraformaldehyde in 0.1 M phosphate buffer. The brain was then removed and placed in 4% paraformaldehyde buffer at 4 °C to fix overnight. After fixation, the brain was cryoprotected in 30% sucrose at 4 °C. Sections were cut at 40 or 50 μm, then collected for confocal imaging. Mice with missed injections or cannula locations were excluded.

Real-time place preference. Mice were placed in a custom made behavioral arena, a plexiglass box (length 50 cm × width 50 cm × height 50 cm), for 10 min. We randomly assigned one side of the chamber as the stimulation side and the counterbalance chamber as the un-stimulation side. Mouse was placed in the no-stimulated side at the onset of the experiment and 20-Hz blue laser was delivered to the LDT when the mouse each time crossed to the stimulated side until it crossed back into the un-stimulation side. The real time place preference location pots and total time in the stimulated side were recorded and counted via MED behavioral recorded systems.

Immunohistochemistry and imaging. Mice were perfused with saline followed by 4% paraformaldehyde in 0.1 M phosphate buffer. The brain was then removed, fixed for 4–6 h, and cryoprotected in 30% sucrose at 4 °C. Sections (40 μm) were cut on a microtome. After rinsing with 0.3% Triton-X 100 (vol/vol) in 0.1 M PBS (30 min) or ice-cold methanol (10 min) and blocking with 10% (wt/vol) normal bovine serum for 1 h at room temperature, sections were incubated with the following primary antibodies (12–24 h at 4 °C): anti-GFP (1:800, rabbit, Chemicon), anti-GAD67 (1:500, mouse, Millipore), anti-GAD65/67 (1:400, rabbit, Abcam), anti-Fos (1:2,500, rabbit, Calbiochem), anti-PV (1:1,500, mouse, Sigma), anti-PV(1:500, Gp, SYSY195004), anti-SOM (1:100, rat, Millipore MAB584), and anti-SOM (1:200, rabbit, Abcam ab64053). After rinsing, sections were incubated with fluorophore-conjugated secondary antibody for 2 h at room temperature (1:1,000; Millipore). Antibodies were diluted in phosphate-buffered saline containing 4% BSA and 0.2% Triton X-100. For c-Fos quantification, mice were exposed to TMT for 10 min, perfused for 1.5 h, and sections cut as described above. After anti-Fos immunohistochemistry, nuclei were stained with DAPI, and confocal images were captured using a 20× objective (Olympus FV-500 or FV-1200).

Preparation of acute slices and electrophysiology. C57 and GAD67-GFP mice were anesthetized with sodium pentobarbital and then perfused with ice-cold oxygenated (95% O_2 and 5% CO_2) aCSF. After decapitation, the brain was quickly removed and placed in ice-cold aCSF containing (in mM): 110 choline-Cl, 2.5 KCl, 0.5 $CaCl_2$, 7 $MgCl_2$, 1.3 NaH_2PO_4, 25 $NaHCO_3$ and 10 glucose. Coronal slices (300 μm) containing the LDT complex were cut on a vibratome (Microm HM 650V), and then allowed to recover in aCSF. Whole-cell patch-clamp recordings were made using an Axon 200B patch-clamp amplifier and 1322A interface (Axon Instruments) at room temperature with a recording solution containing (in mM): 125 NaCl, 2.5 KCl, 2 $CaCl_2$, 1.3 $MgCl_2$, 1.3 NaH_2PO_4, 25 $NaHCO_3$ and 10 glucose saturated with 95% O_2 and 5% CO_2. The electrodes were made from borosilicate glass pipettes (Sutter Instruments) with resistances in the 3–5 M range. The internal solution contained (in mM): 125 potassium gluconate, 15 KCl, 10 HEPES, 4 $MgCl_2$, 4 Na_2-ATP, 0.3 Na_2-GTP, and 0.2 EGTA. To record evoked excitatory postsynaptic currents, GABAergic transmission was blocked by 100 μM picrotoxin in the bath. Signals were filtered at 2 kHz, sampled at 10 kHz, and analyzed using Clampex 8.2 (Axon Instruments). Blue laser light (473 nm, 20 Hz) was delivered through a 200-μm diameter optic fiber positioned at the slice surface over the recorded neuron. After recording, slices were fixed with 4% paraformaldehyde in 0.1 M PBS for immunohistochemical staining.

***In vivo* optetrode recording.** Modified drivable electrode arrays were implanted dorsally to the LDT. Electrode arrays consisted of seven nichrome tetrodes of four thin entwined wires (California Fine Wire) and an optical fiber (100 μm) was glued to the middle of the bundle of seven tetrodes. The micro-wire bundle was attached to a micro-drive. Two EEG wires, two EMG wires, and one ground wire were soldered to a 32-channel connector (Omnetics Connector). Mice were allowed to recover for at least 5 d, then the electrode arrays were connected to a 32-channel preamplifier head-stage (Plexon). Mice were recorded for two sessions per day and electrodes were advanced ~60 μm at the end of each session. 24 h after recording the activity of a LDT neuron in response to light stimulation of ChR2-expressing terminals in the LHb, TMT was given to examine the firing pattern of the same neuron recorded a day before. During sessions, all signals recorded from each tetrode were amplified, filtered between 0.1 Hz and 10 kHz, and spike waveforms were digitized at 40 kHz. Spikes were sorted using the software Offline sorter (Plexon). Units were accepted only if a distinct cluster was visible in a two-dimensional plot of the largest two principal components.

Statistics. No statistical methods were used to pre-determine sample sizes but our sample sizes are similar to those generally employed in the field. All data were randomly collected. Data distribution was assumed to be normal but this was not formally tested. All values are presented as the mean ± s.e.m. The one or two-way ANOVA test, Mann-Whitney U-test, Kruskal-Wallis H test, paired *t* test, or unpaired Student's *t* test were used for group differences as appropriately, and calculated with SPSS 16.0.

A **Supplementary Methods Checklist** is available.